# Polymerization Properties of a Heterogeneous Ziegler−Natta Catalyst Modified by a Base: A Theoretical Study

**Michael Seth and Tom Ziegler***

*Department of Chemistry, University of Calgary, University Drive 2500, Calgary, AB T2N-1N4, Canada*

*Received February 20, 2003; Revised Manuscript Received June 17, 2003*

ABSTRACT: The effects of an external base (tetrahydrofuran, THF) on the ethylene polymerization properties of the $TiCl_4/MgCl_2$ heterogeneous Ziegler−Natta catalyst are examined using density functional methods. THF is found to bind to all of the proposed active sites and most strongly to those formed from $TiCl_3$. THF is also found to bind to the aluminum−alkyl compounds that may be present, and an analysis of equilibrium concentration distributions shows that the most common place for a THF to bind is to an aluminum−alkyl monomer or a $TiCl_3$-based site. The polymerization and termination mechanisms of the remaining sites are examined. It is found that the binding of an ethylene molecule to the site is weakened, and the barrier to insertion of that ethylene molecule into the Ti−C bond is increased by the presence of a THF molecule. However, the polymer produced by each site is expected to have a higher molecular weight than in the absence of THF because the barrier to termination is increased even more than that of insertion by the addition of the base.

## 1. Introduction

Lewis basic compounds such as alcohols, ethers, esters, and ketones are often included in preparations of heterogeneous Ziegler−Natta catalysts. These bases are divided into two types: internal and external. Internal bases are added as the catalyst support is being prepared or perhaps as the transition metal halide is added. It is generally believed that these bases improve the properties of the support somehow either through "activation" by causing a greater number of undercoordinated Mg atoms to become exposed and/or by selectively "deactivating" it by occupying select sites that otherwise would be occupied by metal atoms.[1,2]

External bases are added at a later stage in the catalyst synthesis, usually with the aluminum−alkyl activator. This base has a significant effect on the kinetics of a given catalyst, is usually deactivating, and in the case of propylene polymerization greatly increases the stereospecificity of the reaction.[1−3] These effects are usually explained by proposing that the base coordinates to certain types of active site selectively, displaces internal bases, and/or influences the behavior of the Al cocatalyst.[1−4]

A number of theoretical studies have been applied to the problem of understanding the operation of Ziegler−Natta catalysts.[5−31] A few of these studies[18,22,26] have considered the role of a base, but in all cases, the base is assumed to be coordinated to the surface of the support material.

In this study, we examine the effect of an external Lewis base coordinating to the transition metal atom of the active site or to the activator. The particular catalyst chosen is that formed from $TiCl_4$ supported on $MgCl_2$ with $Al(C_2H_5)_3$ ($AlEt_3$) as the activator. A wide range of compounds have been used as external bases including ethers, diethers, ketones, esters, and amines.[3,32] We have decided to study the action of one base, tetrahydrofuran (THF), in detail. As an ether, THF may coordinate to acidic sites present in the catalyst but will be otherwise unreactive (unlike alcohols for example[3]). It is a relatively small molecule and has little conformational freedom, preventing the calculations from becoming too demanding. Many of the electron donors in common use are significantly larger molecules such as aromatic esters or diethers.[4,32,33] THF may not be a particularly good model of these types of electron donors as they are rather more flexible and have two oxygen atoms capable of coordinating to an available acidic atom. Although external bases are often used to improve the stereoselectivity of Ziegler−Natta catalysts only the homopolymerization of polyethylene is considered in the present study in order to keep the discussion from becoming too complicated. With the results of this work and the previous study[31] in hand, calculations aimed at the polymerization of higher α-olefins are underway in our laboratory.

The structures of the active sites of $TiCl_4/MgCl_2$ catalysts are not known with certainty, though a number of experimental studies have provided some insight.[34−39] Several possible structures have been proposed.[17,40,41] Each structure has as its starting point the surface of $MgCl_2$ that is exposed when it is cut along a given plane. When all of the possible exposed planes are examined it turns out that only two types of low energy Mg environments are commonly encountered, one where Mg is five coordinate (e.g., along the (100), (101), and (104) cuts), and one where it is four coordinate (e.g., along the (110) cut).[1,10] Three possible active site structures have been proposed by placing $TiCl_4$ molecules onto the surfaces so as to form Cl−Mg and Ti−Cl bonds between $TiCl_4$ and the undercoordinated surface atoms.[17,40,41] The three structures, denoted previously as the slope site, Corradini site, and edge site,[31] are illustrated in Figure 1. It should be noted that in each structure in Figure 1 the active site is formed from a $TiCl_2C_3H_7$ molecule on the surface, and the particular cuts chosen are the (101) cut (Figure 1a) and the (110) cut (Figure 1b,c).

In an earlier publication we considered the polymerization of ethylene at each of these sites with the Ti atom in the +4, +3, or +2 oxidation states.[31] In this

10.1021/ma0301247 CCC: $25.00 
Published on Web 08/02/2003

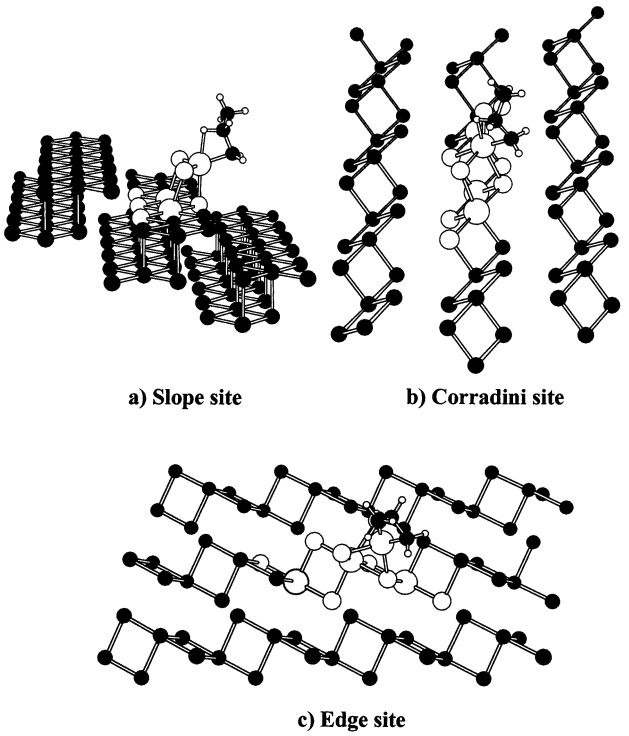


**Figure 1.** Active site models used. With the exception of the propyl chain carbon atoms, all atoms colored black are described using molecular mechanics in the QM/MM scheme.

work we will consider the same series of sites. In ref 31, it was found that $TiCl_4$ has such a low binding energy (BE) to $MgCl_2$ that entropic effects will push the equilibrium of the reaction

$$TiCl_4(ad) \rightleftharpoons TiCl_4(g) \qquad (1)$$

where $TiCl_4$(ad) is a molecule of titanium tetrachloride adsorbed on a $MgCl_2$ surface, strongly to the right. As a consequence, we proposed alternative models of the active site where $TiCl_2$ forms the surface onto which the active site is bound as suggested by recent model experiments.[37−39] Since the structure of crystalline $TiCl_2$ is very similar to that of $MgCl_2$ ,[42] the same three sites could be predicted to form on the alternative surface.

The sites formed by a $TiCl_4$ molecule in a Corradini site and by a $TiCl_2$ molecule in any site do not have the necessary structural features to be active catalysts.[31]

The following sites were retained as possible models of the active site in the $TiCl_4/MgCl_2$ catalyst: $TiCl_4$ in slope and edge sites on $TiCl_2$; $TiCl_3$ at slope, edge, and Corradini sites on both $MgCl_2$ and $TiCl_2$. In previous work, it was found that calculations involving the edge site on $TiCl_2$ converged very poorly. After some experimentation, a $MgCl_2$ model of the surface where only the Mg atom directly below the edge site was exchanged with a $Ti^{2+}$ ion was found to give essentially identical results to the pure $TiCl_2$ surface.[31] This convergence behavior of calculations utilizing this model was relatively good. It was therefore adopted in all calculations of the edge site on "$TiCl_2$".

The discussion will take two parts. After the computational details are described in the next section, the binding of THF to each of the sites and to $AlEt_3$, $AlClEt_2$, $AlCl_2Et$, and $AlCl_3$ will be discussed. In the second half, the steps in the polymerization at the sites with a THF molecule added will be considered.

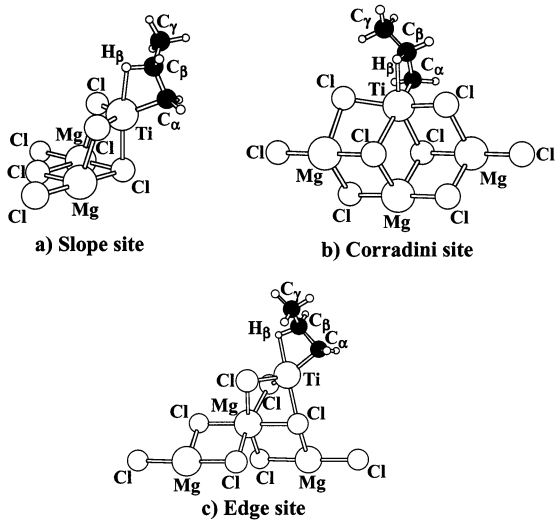


**Figure 2.** Detail of QM part of the active site models.

## 2. Computational Details

The catalyst active site, THF, and all aluminum compounds were described using density functional theory (DFT). A combined quantum mechanical molecular mechanical (QM/MM) approach was used to describe the surfaces to which the active sites are attached. The particular functional used in all DFT calculations was made up of the exchange correction given by Becke[43] and the correlation correction of Perdew[44] with the Vosko, Wilk, and Nusair parametrization of the electron gas.[45] All calculations described in this paper were performed using the ADF program.[46−50]

The MM part of the QM/MM calculations is somewhat different to that utilized in the previous work.[31] With the addition of THF the active site becomes significantly larger and it might be expected that parts of the surface more distant from the Ti atom than were previously considered may have some influence on the activity of the site. To make allowance for this the MM part of the surface was expanded considerably to include the two triple layers on either side on the one where the Ti is bound. The new surface models have formulas $Mg_{24}Cl_{48}$ for the (110) surface and $Mg_{36}Cl_{72}$ for the (101) surface. See Figures 1 and 2. The geometric parameters of the atoms in the surface were frozen at the bulk experimental values of $a = 3.640$ Å and $c = 17.673$ Å for $MgCl_2$ [51] and $a = 3.561$ Å and $c = 5.875$ Å for $TiCl_2$.[42] In the previous study, it was shown that freezing the $MgCl_2$ surface had only a small effect on the active site to surface binding energies.[31] It should be noted that the stacking of the triple layers is different between $MgCl_2$ and $TiCl_2$ with the former following a ABCABC... pattern and the latter an AAA... pattern. The function of the MM atoms in this work is simply to provide steric bulk through nonbonding interactions. Therefore, only the parameters used to simulate van der Waals type interactions were included. A mechanical embedding approach was chosen and no polarization of the wave function by the environment was included. To improve clarity, none of the MM atoms will be shown on all figures except Figure 1.

The geometric parameters of all optimized stuctures can be found in the Supporting Information.

All calculations including $TiCl_3$ or $TiCl_2$ were spin-unrestricted. The Ti atoms in the $TiCl_3$ environments were assumed to have one unpaired electron, and the Ti atoms that were part of the surface $TiCl_2$ were assumed to have two unpaired electrons.

A valence triple-ζ Slater type orbital (STO) basis set was applied to the Ti of the active site while for the Mg, Al, Cl, C, O, H, and surface Ti atoms double-ζ basis sets were used with the exception that the 3d shell of the Ti is described with a triple-ζ set. In addition, the Mg, Al, Cl, O, and C basis sets are supplemented by one 3d polarization function and the H basis set includes a 2p polarization function. The molecular

density and the Coulomb and exchange potentials were fit using an auxiliary s,p,d,f, and g set of STO functions[52] centered on each nucleus. The core definitions used to decide which orbitals to keep frozen were [Ne] for the active site Ti, the Cl, the Al, and the Mg atoms, [He] for C and O, and [Ar] for the surface Ti. The van der Waals parameters of the MM parts of the embedded cluster calculations were taken from the TRIPOS force-field.[53] When TRIPOS did not include the required data parameters were taken from the universal force-field[54] (UFF).

The convergence criteria for geometry optimizations were 0.0001 au in the energy and 0.001 au $Å^{-1}$ or au $rad^{-1}$ in the gradient. The integration parameter used was 5.0. Transition states were located by varying the $C_1$ to $C_\alpha$ bond distance (in the case of the monomer insertion transition states), the difference between the $C_\beta$ to $H_\beta$ and $C_1$ to $H_\beta$ bond distances (in the case of chain transfer with the monomer), and the difference between the $C_\beta$ to $H_\beta$ and Ti to $H_\beta$ bond distances (in the case of $\beta$-H elimination). The transition states were taken to be at the geometry where the energy was a maximum with respect to variations in the chosen parameter and all forces were less than the quoted tolerances.

From the structures of the slope and edge sites given in Figure 2, parts a and c, it is apparent that the Ti atom in these sites may be approached from two directions: either from directly perpendicular to the surface or parallel to the surface and from the opposite side to where the bridging Cl atoms sit. On many occasions in this study, structures or reactions will be differentiated depending upon which of these two sides the participating species lie. To keep clear just what is being discussed the side of the active sites that is approached in a perpendicular directions with respect to the surface will be referred to as the "front" side and the side of the active sites that is approached in a direction that is parallel to the surface will be labeled the "back" side of the site.

## 3. Binding of THF to the Active Site and to $AlEt_xCl_{3-x}$ ($x = 0.3$)

**3.1. Coordination of THF to the Active Site.** The first topic that will be considered is the binding of the THF molecule to each of the proposed active sites. For the sake of comparison, the binding of THF to free $TiCl_4$, $TiCl_3$, $TiCl_3Pr$, and $TiCl_2Pr$ will also be discussed. The BEs of one or two THF molecules coordinated to each of the sites and to the isolated Ti molecules are listed in Table 1. The optimized geometries of the $TiCl_3$-based structures on $MgCl_2$ and the $TiCl_4$-based geometries on $TiCl_2$ modified by one or two THF molecules are given in Figures 3−5. The structures of the $TiCl_3$-based sites on $TiCl_2$ are not shown as they are similar to those of the sites on $MgCl_2$. This policy will be used throughout this paper. The $TiCl_4$-based slope and edge sites have two nonbridging Cl atoms, and it is assumed that both of these are replaced by alkyl groups upon activation meaning that these two active sites include two propyl groups. Note that the $TiCl_4$-based edge site on $TiCl_2$ has a six-coordinate Ti atom once a THF is added since the Ti atom forms an additional bond with a Cl surface atom. This is in contrast to the case where the THF is absent. In this case the Ti is four coordinate, and no Ti to surface Cl bond is present. However, a similar six-coordinate structure is formed at the same site once ethylene $\pi$-complexes with the Ti atom.[31] Thus, it would appear that Ti prefers to be either four- or six-coordinate.

It is clear from the results in Table 1 that the most important factors in determining how strongly the first THF molecule binds to an active site are mostly steric rather than electronic in nature. The species based on $TiCl_4$ are more acidic than those based on $TiCl_3$. However, the binding energies of THF to the former (2−16 kcal/mol) are in all cases much less than those to the latter (16−27 kcal/mol) due to the higher steric congestion at the $TiCl_4$ sites. The BE of THF to isolated $TiCl_3$ falls into the middle of the range of the energies found for the $TiCl_3$-based sites and the BE of THF to $TiCl_4$ is similarly in the middle of the range of energies found for the $TiCl_4$-based sites. It would therefore seem that the surface to which the active site is bound does not strongly influence the THF-active site interactions though it does have some effect (see below). The replacement of a Cl atom in the isolated Ti molecules with a propyl ligand leads to a small decrease in THF binding. There is a systematic difference between the $E_B$ of THF to the front and back side of the sites that have two possible coordination sites (the $TiCl_3$-based edge and slope sites; see Figure 4). In all cases the BEs to the front are greater than those of THF to the back of the same site. This is presumably also a steric effect as coordination to the back face places the THF closer to the surface than if it was bound to the front face.

**Table 1. Binding Energies of THF to Active Sites**

| site | type | face[b] | BE |
|---|---|---|---|
| $TiCl_4$ | free | | 9.3 |
| $TiCl_3$ | free | | 24.7 |
| $TiCl_3Pr$ | free | | 9.1 |
| $TiCl_2Pr$ | free | | 21.1 |
| | $MgCl_2$ Surface | | |
| $TiCl_2Pr$ | slope | front | 27.7 |
| $TiCl_2Pr$ | slope | back | 23.2 |
| $TiCl_2Pr$ | slope | front + back | 31.2 |
| $TiCl_2Pr$ | slope | back + back | 35.7 |
| $TiCl_2Pr$ | Corradini | front | 21.8 |
| $TiCl_2Pr$ | edge | front | 24.7 |
| $TiCl_2Pr$ | edge | back | 18.4 |
| $TiCl_2Pr$ | edge | front + back | 31.5 |
| $TiCl_2Pr$ | edge | back + back | 40.4 |
| | $TiCl_2$ Surface | | |
| $TiCl_2Pr_2$ | slope | front | 2.5 |
| $TiCl_2Pr_2$ | slope | back | 10.0 |
| $TiCl_2Pr_2$ | edge | front | 7.1 |
| $TiCl_2Pr_2$ | edge | back | 16.1 |
| $TiCl_2Pr$ | slope | front | 21.1 |
| $TiCl_2Pr$ | slope | back | 16.4 |
| $TiCl_2Pr$ | slope | front + back | 21.2 |
| $TiCl_2Pr$ | slope | back + back | 25.3 |
| $TiCl_2Pr$ | Corradini | front | 20.2 |
| $TiCl_2Pr$ | edge | front | 24.4 |
| $TiCl_2Pr$ | edge | back | 19.9 |
| $TiCl_2Pr$ | edge | front + back | 35.9 |
| $TiCl_2Pr$ | edge | back + back | 37.0 |

[a] Energies in kcal/mol. [b] The side of the active site to which THF is complexed.

The $TiCl_3$-based slope and edge sites each have two vacant sites in the coordination sphere of Ti. Therefore, the structures of these sites with a pair of coordinated THF molecules were calculated. Two arrangements of ligands for each site were considered: one with the propyl group on the front face of the site and one with it on the back of the site, leaving the remaining two coordination sites for THF. The total BE of the two THF molecules to each site are listed in Table 1. A little surprisingly, the binding energies of the first and second THF molecules are significantly nonadditive. There appears to be a preference for binding the first THF molecule to the front of the site but the binding of two THF molecules to the back side of the site is more favorable than one on the front side and one on the back side.

**3.2. Coordination of THF to the Activator.** Ziegler−Natta reactions typically use some kind of alumi-

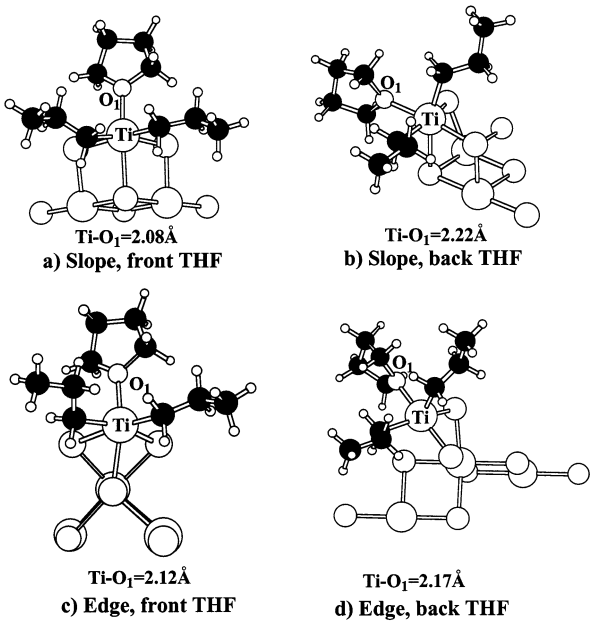


**Figure 3.** $TiCl_4$-based sites modified by a THF molecule.

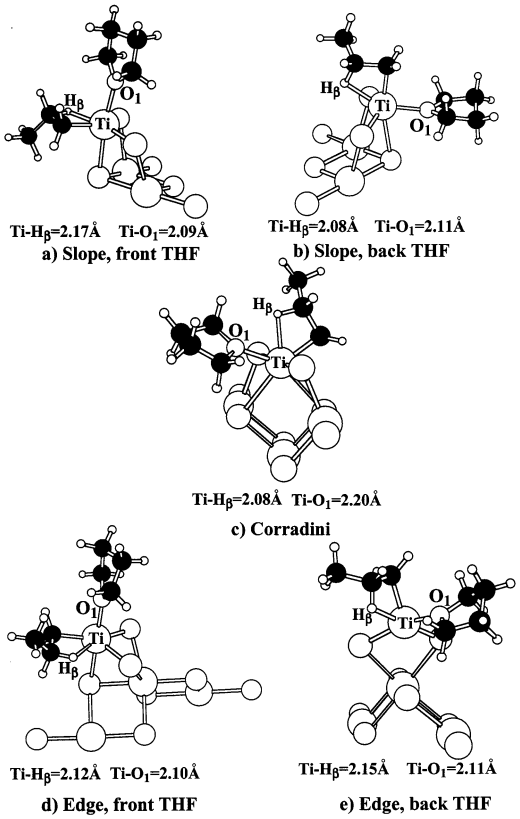


**Figure 4.** $TiCl_3$-based sites modified by a THF molecule.

num−alkyl compounds as an activator. It is believed that the function of this activator is to replace one of the Cl atoms bonded to Ti with an alkyl chain creating the active site. Aluminum−alkyls are acidic and may form complexes with bases such as THF in competition with the Ti atoms of the active site.

To investigate this possibility the structures of a number of aluminum−alkyl−THF complexes were calculated including the 1:1, 1:2, and 2:1 THF:$AlEt_xCl_{x-3}$ ($x = 1-3$) systems. The 1:2 complex is that derived from the coordination of a THF molecule to the dimer usually formed by these types of aluminum compounds. Some

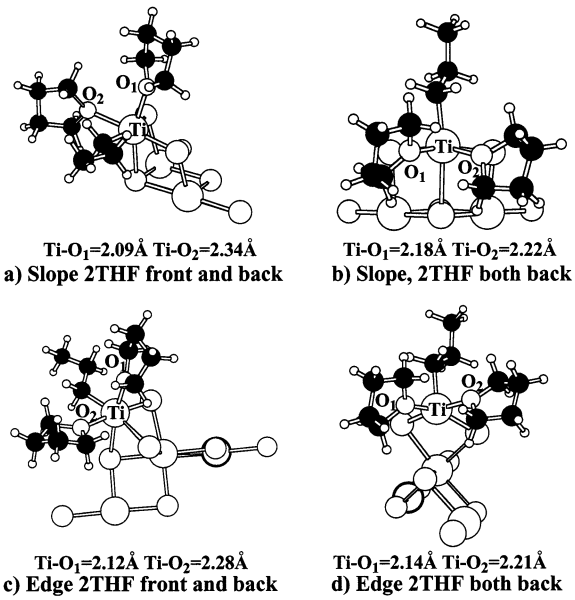


**Figure 5.** $TiCl_3$-based sites modified by two THF molecules.

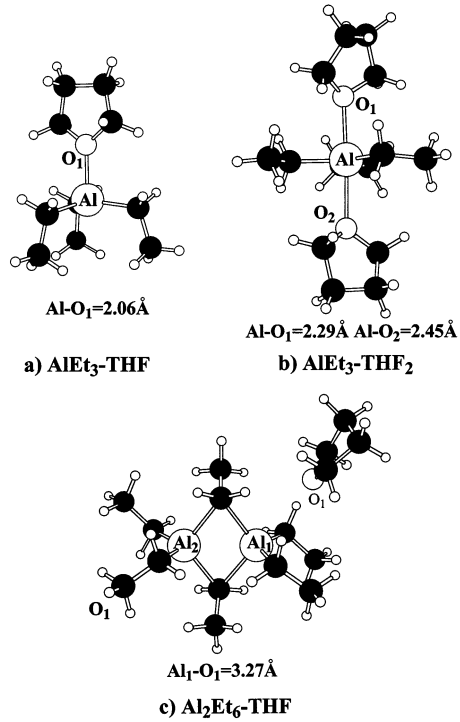


**Figure 6.** Complexes of THF and $AlEt_3$.

calculations of the 2:2 complexes (two THF molecules coordinating to an aluminum−alkyl dimer) were attempted but two 1:1 complexes were always obtained. Cl atoms (when present) were chosen to bridge the aluminum atoms since test calculations found this arrangement to be more stable than the alternative with bridging ethyl groups. The BEs of THF to the various aluminum−alkyl molecules are listed in Table 2 and the structures of the 1:1, 1:2, and 2:1 complexes of THF with $AlEt_3$ are shown in Figure 6.

The data in Table 2 follow the trends that would be expected. Aluminum prefers to be in a tetrahedral environment and as a result a single THF binds strongly to a monomeric aluminum compound but only weakly to the dimer. The complexation energy of a second THF to a monomer is equal to the difference between the BE

**Table 2. Binding Energies of THF to the Activator**

| Al compound | no. of THF | BE |
|---|---|---|
| $AlEt_3$ | 1 | 16.6 |
| $AlEt_2Cl$ | 1 | 20.3 |
| $AlEtCl_2$ | 1 | 25.5 |
| $AlCl_3$ | 1 | 30.0 |
| $AlEt_3$ | 2 | 20.9 |
| $AlEt_2Cl$ | 2 | 28.2 |
| $AlEtCl_2$ | 2 | 32.7 |
| $AlCl_3$ | 2 | 41.8 |
| $Al_2Et_6$ | 1 | 2.4 |
| $Al_2Et_4Cl_2$ | 1 | 8.6 |
| $Al_2Et_2Cl_4$ | 1 | 12.5 |
| $Al_2Cl_6$ | | |

[a] Energies in kcal/mol.

of two and one THF molecules to the same aluminum compound or 4.3, 7.9, 7.2, and 11.8 kcal/mol for $AlEt_3$, $AlEt_2Cl$, $AlEtCl_2$, and $AlCl_3$ respectively. These are also rather small BEs.

Replacing the ethyl groups successively with Cl atoms increases the Al−THF interaction. This is also to be expected as Cl is sterically smaller and more electron withdrawing than the ethyl group, leading to a more acidic Al atom.

The BE of a single THF to $AlCl_3$, $AlEtCl_2$, or $AlEt_2Cl$ is similar to that of THF to the $TiCl_3$-based sites. The BE of THF to the other aluminum−alkyl species is more similar to the BE of THF to the $TiCl_4$-based sites.

The equilibrium geometries of the THF−aluminum−alkyl complexes shown in Figure 6 are fairly unremarkable. Two points are worth noting. First, in the Al−$(THF)_2$ systems, the THF ligands prefer to be trans as shown in Figure 6. Attempts to optimize structures with the two THF molecules cis gave higher energy geometries corresponding to a Al−THF complex with a weakly associated THF. Second, in the more crowded Al−$(THF)_2$ and $Al_2$−THF structures the Al−O bond distances are rather long. As ethyl groups are replaced with Cl atoms, these distances become shorter.

**3.3. Equilibrium Distributions of Catalyst/Activator/THF Mixtures.** In the previous two sections, calculations of the binding energies of THF to the catalyst and activator were described. In the real catalytic system, each constituent can participate in a number of reactions, and it is not easy to decide from the BEs how much of each species is present. We do not attempt to give a comprehensive analysis of all possible reactions of the activator, the active site, and THF since many can be postulated and such an analysis is beyond the scope of this paper. What will be presented are some calculated equilibrium concentrations derived using the BEs already discussed.

The procedure that was used to calculate equilibrium concentrations is as follows. Given the change in Gibbs free energy of a reaction $\Delta G$, the equilibrium constant of that reaction can be calculated from[55]

$$K = e^{-\Delta G/RT} \tag{2}$$

The reaction energies given in this work are of course not Gibbs free energies but instead correspond to internal energy changes at 0 K ($\Delta U(0)$). The remaining contributions to $\Delta G$ can be calculated[56,57] in a procedure requiring (among other things) harmonic vibrational frequencies of each molecule. The computation of vibrational frequencies is a computationally very demanding task in this case given the number of molecules concerned and their large sizes. It should also be noted that some of the molecules include floppy alkyl chains whose vibrations are likely to be rather anharmonic, making any analysis based on harmonic vibrational frequencies rather unreliable. Only semiquantitative results are required for the present discussion, and it was therefore decided to use more approximate methods to obtain values for $\Delta G$.

**Table 3. Free Energies of Coordination between THF and Active Sites**

| site | type | face[b] | $\Delta G$ |
|---|---|---|---|
| | | $MgCl_2$ Surface | |
| $TiCl_2Pr$ | slope | front | −12.6 |
| $TiCl_2Pr$ | slope | back | −8.1 |
| $TiCl_2Pr$ | slope | front + back | −1.0 |
| $TiCl_2Pr$ | slope | back + back | −5.5 |
| $TiCl_2Pr$ | Corradini | front | −6.7 |
| $TiCl_2Pr$ | edge | front | −9.6 |
| $TiCl_2Pr$ | edge | back | −3.3 |
| $TiCl_2Pr$ | edge | front + back | −1.3 |
| $TiCl_2Pr$ | edge | back + back | −10.2 |
| | | $TiCl_2$ Surface | |
| $TiCl_2Pr_2$ | slope | front | 12.6 |
| $TiCl_2Pr_2$ | slope | back | 5.1 |
| $TiCl_2Pr_2$ | edge | front | 8.0 |
| $TiCl_2Pr_2$ | edge | back | −0.9 |
| $TiCl_2Pr$ | slope | front | −6.0 |
| $TiCl_2Pr$ | slope | back | −1.3 |
| $TiCl_2Pr$ | slope | front + back | 9.0 |
| $TiCl_2Pr$ | slope | back + back | 4.9 |
| $TiCl_2Pr$ | Corradini | front | −5.1 |
| $TiCl_2Pr$ | edge | front | −9.3 |
| $TiCl_2Pr$ | edge | back | −4.8 |
| $TiCl_2Pr$ | edge | front + back | −5.7 |
| $TiCl_2Pr$ | edge | back + back | −6.8 |

[a] Energies in kcal/mol. [b] The side of the active site to which THF is complexed.

Although Ziegler−Natta reactions are carried out in both the gas phase and in solution/slurry, it was assumed for the present purposes that the reactions were in the gas phase. Therefore, to convert the changes in internal energy $\Delta U(0)$ to enthalpies it was possible to approximate the $p\Delta V$ contribution by $\Delta nRT$ where $\Delta n$ is −1 for a simple bimolecular addition (A + B → AB). At 350 K, a temperature within the normal range used in Ziegler−Natta catalysis,[3] this corresponds to −0.7 kcal/mol. The entropy change for bimolecular addition reactions is relatively large and negative and from our experience is generally on the order of −45 cal $mol^{-1}$ $K^{-1}$. At 350 K, this corresponds to a $-\Delta ST$ of +15.8 kcal/mol. Nonzero kelvin temperature effects were neglected as they are small compared to the accuracy expected for these approximate corrections. The overall correction to each $\Delta U$ to give the corresponding $\Delta G$ was therefore +15.1 kcal/mol. The derived $\Delta G$ values are given in Tables 3 and 4. Some of the reactions listed in Tables 3 and 4 involve the addition of two THF molecules to the activator or an active site. In these cases a correction twice as large was applied to convert $\Delta U(0)$ into $\Delta G$.

The dimerization reactions of the aluminum species are also included in the analysis. The association energies of the dimers of $AlEt_3$, $AlClEt_2$, $AlCl_2Et$, and $AlCl_3$ were calculated. It has been shown that DFT methods underestimate the strength of electron deficient bonds like Al−Cl−Al and Al−$CH_3$−Al bridges.[58] From a comparison of the calculated and experimental[59,60] dimerization energies of $AlCl_3$ and $Al(CH_3)_3$, it was determined that the functional/basis set combination used here underestimate Al−Cl−Al and Al-Et-Al

**Table 4. Free Energies of Coordination between THF and Aluminum Activator**

| aluminum species | no. of THFs | $\Delta G$ |
|---|---|---|
| $AlEt_3$ | 1 | −1.5 |
| $AlEt_2Cl$ | 1 | −5.2 |
| $AlEtCl_2$ | 1 | −10.4 |
| $AlCl_3$ | 1 | −14.9 |
| $AlEt_3$ | 2 | 8.3 |
| $AlEt_2Cl$ | 2 | 2.0 |
| $AlEtCl_2$ | 2 | −2.5 |
| $AlCl_3$ | 2 | −11.6 |
| $Al_2Et_6$ | 1 | 12.7 |
| $Al_2Et_4Cl_2$ | 1 | 6.5 |
| $Al_2Et_2Cl_4$ | 1 | 2.6 |
| $Al_2Cl_6$ | 1 | −2.7 |

[a] Energies in kcal/mol.

**Table 5. Free Energies of Association of Aluminum Activator**

| aluminum species | $\Delta G$ |
|---|---|
| $AlEt_3$ | −4.6 |
| $AlEt_2Cl$ | −16.1 |
| $AlEtCl_2$ | −14.2 |
| $AlCl_3$ | −13.8 |

[a] Energies in kcal/mol. [b] Adjusted values. See text.

bonds by 3.0 and 3.4 kcal/mol respectively. Appropriate corrections were applied to all of the dimerization energies of the aluminum compounds listed in Table 5.

An enormous range of reaction conditions are used in Ziegler−Natta processes making it difficult to choose a representative set to apply here. It was decided to take the conditions set out by Matos and co-workers in their recent paper[61] which were chosen to be "in accordance with actual industrial conditions"[61] and which give numbers that are easy to work with. Molarities taken from the middle of their chosen ranges are: 1.2, 1.8, and 1.4 mol/m$^3$ for Ti, aluminum compounds, and external base, respectively,[61] given a density of $MgCl_2$ of 2.316 g/cm$^3$.[62] No general agreement as to the oxidation state distribution of Ti has been reached in the literature. In our model we arbitrarily choose to have an even distribution of 0.4, 0.4, and 0.4 mol/m$^3$ of the +4, +3, and +2 oxidation states. The +2 oxidation state is unreactive toward olefin polymerization in any of the models we are examining and therefore will not be considered further.

Since the distribution of types of active site is also not known all the Ti(III) sites were treated as one. The reactions Ti(III) + THF → Ti(III)−THF, Ti(III)−THF + THF → Ti(III)−$(THF)_2$, and Ti(IV) + THF → Ti(IV)−THF were assigned $\Delta G$ values of −9, +3, and +3 kcal/mol, respectively, based on the most favorable values from Table 3.

The equilibrium constants obtained from the derived values of $\Delta G$ in combination with the chosen component concentrations provide a system of nonlinear equations which were solved iteratively using a small FORTRAN program written by us. The concentrations of various species depending on the initial composition of the system are given in Table 6.

A number of inferences can be drawn from the data in Table 6. First, these results imply that in the presence of THF almost all Ti(III) sites have a single base coordinated to them while this is so only for a small fraction of Ti(IV) sites. The addition of a normal amount of aluminum−alkyl has little effect on the proportion of Ti atoms to which a THF is coordinated. The aluminum compounds do coordinate THF well enough to significantly reduce the concentration of aluminum−alkyl dimers in favor of aluminum−alkyl−THF complex.

If the binding energies of THF to the aluminum compounds are combined with their respective dimerization energies the following series (in order of increasing exothermicity for the reaction $Al_2R_6$ + 2THF → 2$AlR_3$·THF) is obtained: $AlEt_2Cl$ < $AlEt_3$ < $AlEtCl_2$ < $AlCl_3$. Thus, it would be expected that if the major function of the external base is to coordinate to the activator, then it would become more effective as activation proceeds producing more highly chlorinated aluminum compounds. Alternatively, if the aluminum compounds interfere with some other desirable action of THF, then they would interfere more strongly as activation proceeds.

The last two rows of Table 6 indicate what may happen if a large excess of either THF or $AlCl_3$ is added to the reaction mixture. The second of these two cases is particularly relevant as such a large excess of aluminum activator often is optimal for catalyst performance.[63,64] It appears that a large excess of THF should poison the catalyst as the $TiCl_3$-based sites start to become doubly coordinated and a significant number of the $TiCl_4$-based sites coordinate a THF molecule. Conversely, in the presence of a large excess of $AlCl_3$ many of the $TiCl_3$-based sites have no base coordinated to them at all.

It is difficult to give a precise idea of the likely errors in this analysis given the nonlinear way in which the equilibrium concentrations depend on the calculated energies. Given that the equilibrium constants depend on the exponential of the $\Delta G$ values, relatively small errors in $\Delta G$ can lead to large changes in $K$. To get some idea of the possible errors, the equilibrium distributions were recalculated a few times with a not unreasonable error of 3 kcal/mol added or subtracted from various reaction free energies. The results obtained were not in disagreement with any of the general conclusions expressed in the previous paragraphs. None of the components that were present in very low concentrations (less than $10^{-3}$ mol/m$^3$) became important. None

**Table 6. Equilibrium Distributions of Catalyst/Aluminum Compound/External Base Mixtures**

| initial concn | | | | | final concn | | | | | | | | | |
|---|---|---|---|---|---|---|---|---|---|---|---|---|---|---|
| III | IV | Al | T | Al compn | III | III−T | III−$T_2$ | IV | IV−T | Al | $Al_2$ | Al−T | $Al_2$−T | T |
| 0.0 | 0.0 | 1.8 | 1.4 | $AlEt_3$ | 0.0 | 0.0 | 0.0 | 0.0 | 0.0 | $4.5 \times 10^{-2}$ | 0.67 | 0.42 | 0.0 | 0.98 |
| 0.0 | 0.0 | 1.8 | 1.4 | $AlCl_3$ | 0.0 | 0.0 | 0.0 | 0.0 | 0.0 | $2.1 \times 10^{-5}$ | 0.20 | 1.40 | $3.1 \times 10^{-4}$ | $2.8 \times 10^{-5}$ |
| 0.4 | 0.4 | 0.0 | 1.4 | | 0.0 | 0.39 | $5.6 \times 10^{-3}$ | 0.39 | $5.6 \times 10^{-3}$ | 0.0 | 0.0 | 0.0 | 0.0 | 0.99 |
| 0.4 | 0.4 | 1.8 | 1.4 | $AlEt_3$ | $1.3 \times 10^{-6}$ | 0.40 | $3.9 \times 10^{-3}$ | 0.40 | $3.9 \times 10^{-3}$ | $4.7 \times 10^{-2}$ | 0.73 | 0.30 | 0.0 | 0.69 |
| 0.4 | 0.4 | 1.8 | 1.4 | $AlCl_3$ | $4.9 \times 10^{-2}$ | 0.35 | 0.0 | 0.40 | 0.0 | $2.9 \times 10^{-5}$ | 0.37 | 1.05 | $3.2 \times 10^{-4}$ | $1.6 \times 10^{-5}$ |
| 0.4 | 0.4 | 180 | 1.4 | $AlCl_3$ | 0.26 | 0.14 | 0.0 | 0.40 | 0.0 | $4.5 \times 10^{-4}$ | 89.4 | 1.25 | $6.1 \times 10^{-3}$ | $1.2 \times 10^{-6}$ |
| 0.4 | 0.4 | 1.8 | 140 | $AlEt_3$ | 0.0 | 0.14 | 0.26 | 0.14 | 0.26 | $1.4 \times 10^{-3}$ | $6.5 \times 10^{-4}$ | 1.80 | 0.0 | 137.3 |

[a] All concentrations in mol/m$^3$. [b] III denotes Ti(III). [c] IV denotes Ti(IV). [d] T denotes THF.

of the general trends changed. However, a couple of the minor components (between $10^{-1}$ and $10^{-3}$ mol/m$^3$) did increase significantly in concentrations. In particular, these tests suggest that $AlCl_3$ may be able to compete with the $TiCl_3$-based sites even at lower concentrations of $AlCl_3$ and that in the presence of the less acidic $AlEt_3$ the interaction between the $TiCl_4$-based sites and THF may be strong enough to poison a substantial proportion (25%) of the sites. One possible source of error that at least has a known sign is the basis-set superposition error (BSSE). BSSE results in a slight overestimation of binding energies and may lead to the calculated concentrations of AB species being a little too high relative to separated A and B.

## 4. Mechanistic Details

In this section, the important steps in polymerization of ethylene at the sites with an added THF will be examined. The mechanism was again assumed to be that proposed by Cossee and Arlman.[65−68] The mechanism is made up of four steps. The resting state is composed of a Ti atom with an attached polymer chain and up to four other ligands leaving space for a monomer molecule to approach. An α-olefin occupies this space through $\eta^2$-coordination forming a $\pi$-complex. The two carbons bound to the metal then insert into the Ti−polymer bond via a four-membered cyclic transition state regenerating the resting state with a polymer chain lengthened by one unit. Each of these steps will be studied in turn.

In ref 31, it was found that the Ti to surface Cl bond was relatively weak for the edge sites and was broken in a few cases to facilitate the progress of a reaction. Therefore, the possibility of the $TiCl_4$-based edge site remaining catalytically active even after the addition of a THF molecule due to the breaking of this bond was considered. However, it was found in preliminary calculations that sites of this type with the Ti to surface Cl bond broken were very high in energy. This type of system was not considered further.

**4.1. Resting States.** The resting states of the various possible catalytic sites are the site with an added THF molecule, the growing polymer chain (modeled here by a propyl group), and available space in their coordination sphere for the addition of an ethylene molecule. This limits our discussion to the $TiCl_3$-based slope and edge sites with a single complexed THF molecule. These sites with two THF molecules, the $TiCl_3$-based Corradini site, and the $TiCl_4$-based sites with a single THF molecule all lack an empty coordination site into which an approaching ethylene molecule can go.

Each of the $TiCl_3$-based slope and edge sites has two possible resting states depending on the relative placement of the THF and polymer chain. As was discussed in the previous section, in each case the structure where the THF molecule is at the front side is about 4 kcal/mol lower in energy than when it is at the back side. Therefore, if the barrier between interchange of these two structures is low, then the resting state with the THF molecule on the front side will predominate. It is assumed that this is the case here in order to simplify the comparisons of energy barriers, i.e., the resting state energy used to calculate reaction energies "with respect to the separated site and ethylene" will always be that of the site with THF on the front side irrespective of where it is placed as the ethylene molecule complexes with the Ti atom or reacts with the growing polymer chain.

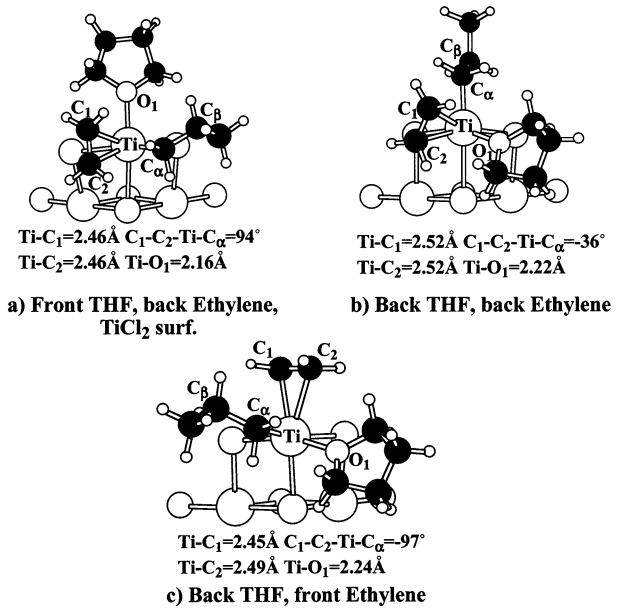


**Figure 7.** $\pi$-Complexes of the slope site.

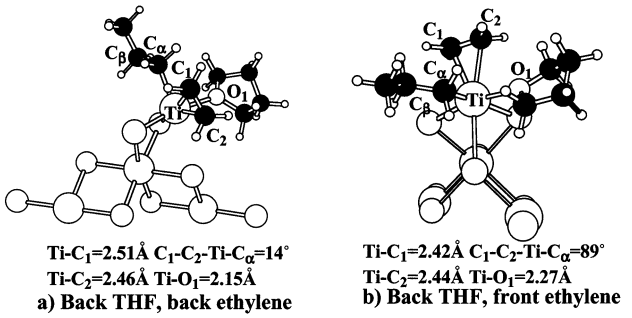


**Figure 8.** $\pi$-Complexes of the edge site.

The only other point of interest with respect to the resting state structures is that they all retain a significant $\beta$-agostic interaction as indicated by the short $H_\beta$−Ti distances shown in Figure 4. Thus, although the THF modified $TiCl_3$-based slope and edge sites have the same coordination number as the unmodified $TiCl_4$-based slope and edge sites (for which the structures without $\beta$-agostic interactions are lower in energy than those where they are present[31]), they behave more like the unmodified $TiCl_3$-based sites when it comes to the formation of $\beta$-agostic interactions. A few structures without the $\beta$-agostic interaction present were optimized and found to be between 1 and 4 kcal/mol higher in energy than the equivalent structure where the interaction was present. Since the structures with and without a $\beta$-agostic interaction are so close in energy it may well be that the polymer chain is most often arranged so that the $\beta$-agostic bond is missing as this situation allows greater conformational freedom and is therefore entropically favored.

**4.2. $\pi$-Complexes.** As a precursor to the polymerization reaction, it is believed that ethylene first forms a $\pi$-complex with the Ti atom. The geometries and energies of the THF-modified sites with an added ethylene molecule therefore were examined. In both site models three positions about the Ti molecule are taken up by Cl atoms which are held in place by the surface. The THF, ethylene, and growing polymer chain fill the three remaining coordination sites thus giving three possible $\pi$-complex structures as the ligands are distributed about the two back side spaces and single front

**Table 7. Energies and Geometrical Parameters of the Polymerization and Chain Transfer Reactions with THF Added**

| site type | | ethylene[c] | THF[d] | $E_\pi$ [e] | $E_{I(\pi)}$ [f] | $E_{I(s)}$ [g] | $E_{T(\pi)}$ [h] | $E_{T(s)}$ [i] |
|---|---|---|---|---|---|---|---|---|
| | | | | $MgCl_2$ Surface | | | | |
| $TiCl_2Pr$ | slope | front | back | −1.4 | 7.4 | 8.7 | 12.3 | 13.6 |
| $TiCl_2Pr$ | slope | back | front | *b* | *b* | 14.6 | *b* | 19.1 |
| $TiCl_2Pr$ | slope | back | back | −3.5 | 5.7 | 9.2 | 11.2 | 14.7 |
| $TiCl_2Pr$ | edge | front | back | 5.1 | 8.4 | 3.2 | 14.5 | 9.4 |
| $TiCl_2Pr$ | edge | back | front | *b* | *b* | 5.7 | *b* | 17.3 |
| $TiCl_2Pr$ | edge | back | back | 2.7 | 6.2 | 3.5 | 13.8 | 11.2 |
| | | | | $TiCl_2$ Surface | | | | |
| $TiCl_2Pr$ | slope | front | back | −8.9 | 3.1 | 12.0 | 8.3 | 17.3 |
| $TiCl_2Pr$ | slope | back | front | −6.4 | 7.6 | 14.0 | 18.8 | 25.2 |
| $TiCl_2Pr$ | slope | back | back | −9.5 | 2.2 | 11.7 | 9.3 | 18.8 |
| $TiCl_2Pr$ | edge | front | back | 6.5 | 9.3 | 2.8 | 16.2 | 9.8 |
| $TiCl_2Pr$ | edge | back | front | *b* | *b* | 3.5 | *b* | 14.8 |
| $TiCl_2Pr$ | edge | back | back | 4.4 | 6.7 | 2.3 | 13.6 | 9.4 |

[a] Energies in kcal/mol. [b] No geometry corresponding to a bound monomer could be found for these sites. [c] The side of the active site to which ethylene is complexed. [d] The side of the active site to which THF is complexed. [e] Complexation energies of ethylene. [f] Ethylene insertion barrier with respect to $\pi$ complex. [g] Ethylene insertion barrier with respect separated monomer. [h] Hydrogen transfer barrier with respect to $\pi$ complex. [i] Hydrogen transfer barrier with respect to separated monomer and site.

side space available. The optimized structures are shown in Figures 7 and 8. Note that the structure of the site on $TiCl_2$ is shown in Figure 7a since the ethylene molecule fell off the equivalent site on $MgCl_2$. The formation energies of the $\pi$-complexes ($E_\pi$) are given in Table 7.

Clearly, ethylene binds rather weakly to these sites. The $\pi$-complexation energies given in Table 7 are all either fairly small and positive or negative, or no structure corresponding to a bound ethylene could be found at all. This last situation applies to the binding of ethylene to the back side when THF is in a back-position. Only one of the four possible site/surface combinations where this situation arises gives a bound ethylene. The ethylene molecule binds more strongly to the edge sites than to the slope sites. This is presumably also a steric effect as the two bridging Cl atoms in the edge site are bound to a single surface Mg or Ti making the site somewhat less crowded than the slope site where each bridging Cl is bound to a separate surface Mg or Ti atom (see Figure 2).

The weak binding of ethylene to Ti is in contrast to what was found for the $TiCl_3$-based sites in the absence of a THF where the complexation energy of ethylene was 9 kcal/mol or higher in all cases.[31] The values of $E_\pi$ given in Table 7 are closer to (though slightly higher) the $\pi$-complexation energies of ethylene to unmodified $TiCl_4$-based sites.[31] It therefore seems that steric effects are the most important factor in determining the relative ability of ethylene to bind to the Ti atom in these sites. The slightly higher $E_\pi$ values for the modified $TiCl_3$-based sites as compared with the unmodified $TiCl_4$-based sites does suggest that the greater ability of Ti in the $TiCl_3$-based sites to donate electron density into the $\pi^*$ orbital of the monomer has a significant but lesser effect.

In section 3.3 it was noted that the reaction A(g) + B(g) → AB(g) almost always involves a significant loss of entropy. Similar statements can be made about the formation of the $\pi$-complex from gaseous ethylene. It would therefore be expected that the $\Delta G$ of the complexation energies will be about 15 kcal/mol more positive than −1 times the values of $E_\pi$ given in Table 7. Note that in this work all binding/complexation energies are positive if the bound system is lower in energy than the separated components, thus the need for the −1 in the previous sentence. Each of the $\Delta G(\pi)$ is likely to be significantly positive. Similarly, in the next sections, if one wishes to considers Gibbs' free energies of activation of the insertion and termination steps, they are likely to be be about 15 kcal/mol more positive than the given barrier heights relative to separated active site and monomer. The Gibbs' free energy of activation with respect to the $\pi$-complex will probably be very similar to the corresponding calculated barrier heights of course.

In terms of geometry, structures where the ethylene molecule is on the more open front side of the active site and are oriented perpendicular to the growing polymer chain were found to be lowest in energy as was the case with the unmodified site.[31] The steric requirements of the back positions force the monomer to be perpendicular to the surface in all cases irrespective of the placement of the propyl group and the THF molecule. The $\pi$-complexes are naturally much more crowded than the resting states and as a result the formation of $\beta$-agostic bonds become energetically unfavorable and Ti−O bond lengths are lengthened by between 0.05 and 0.15 Å upon addition of the ethylene molecule.

**4.3. Polymerization Transition States.** The Cossee−Arlman mechanism postulates that the polymerization of an α-olefin at a Ziegler−Natta catalyst proceeds through a concerted process involving a four-membered transition state made up of the two $sp^2$ carbons from the olefin, the titanium atom, and the first carbon of the growing polymer chain. Transition states of this type were found for all possible arrangements of ethylene, THF, and the growing polymer chain around the $TiCl_3$-based slope and edge sites on $MgCl_2$ and $TiCl_2$. The energies of these transition states with respect to the appropriate $\pi$-complex ($E_{I(\pi)}$) and with respect to the resting state (site with THF in the most energetically favorable position) ($E_{I(s)}$) are given in Table 7. The structures of the transition states along with some geometric parameters are given in Figures 9 and 10.

The $E_{I(\pi)}$ values for those sites which have stable $\pi$-complexes are all between 2 and 8 kcal/mol. The insertion barriers with respect to the separated components show more of a trend in that the barriers for the edge sites are uniformly lower than those of the slope sites and the barriers are higher when the THF molecule is on the front side of the site than when it is on the back side. In addition, the two insertion barriers for each site when the THF molecule is on the back side are very close to each other. The transition states of the edge sites are lower in energy because of the lower

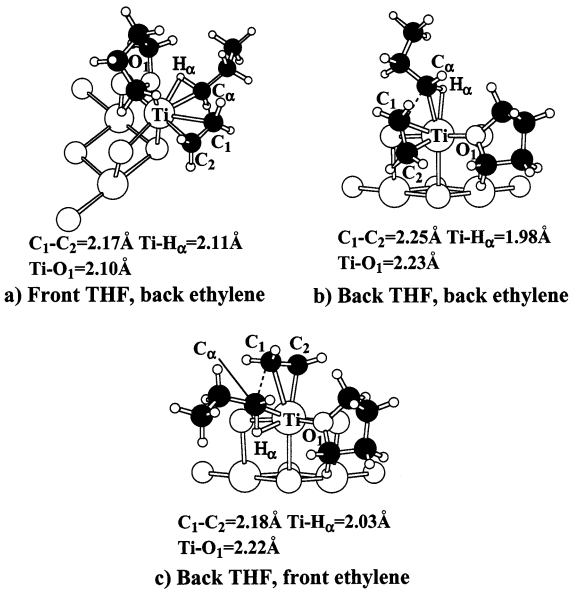


**Figure 9.** Ethylene insertion transition states of the slope site.

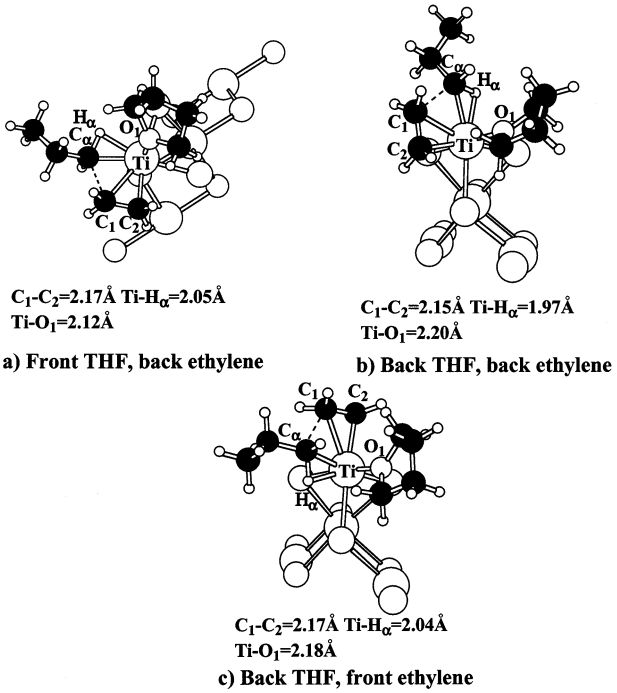


**Figure 10.** Ethylene insertion transition states of the edge site.

amount of crowding about the Ti atom, much like the $\pi$-complexes. α-Agostic interactions are present in all transition states.

Unsurprisingly, the $E_{I(s)}$ values in Table 7 are all significantly higher than the values of the equivalent sites in the absence of THF.[31] This is mainly due to the greater amount of energy required to bring the ethylene molecule into the Ti coordination sphere since the insertion barriers relative to the $\pi$-complex are much lower in the present case than when no THF was present. The values of the barriers are more in line with what was calculated for the $TiCl_4$-based sites without added THF.[31]

**4.4. Termination Transition States.** A number of possible termination mechanisms have been proposed for the classical Ziegler−Natta catalyst.[1] Any or all of these mechanisms may operate under a given set of reaction conditions. It has been found that under the usual polymerization conditions and in the absence of molecular hydrogen, termination by chain transfer with a monomer is the most important termination pathway.[1,69] Computational studies of the $TiCl_4/MgCl_2$ Ziegler−Natta catalyst in the absence of a base also have come to the same conclusion.[14,31]

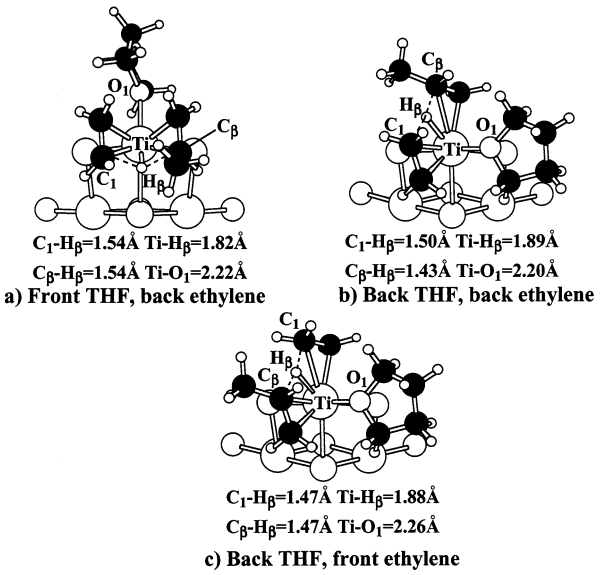


**Figure 11.** Chain transfer with ethylene transition states of the slope site.

As has already been noted, the coordination of a THF molecule to the Ti atom of an active site increases the steric crowding around that site. The transition state geometry of the $\beta$-hydride elimination termination pathway is less sterically demanding than that of chain transfer with the monomer,[69] and it therefore might be expected that the former mechanism may become dominant in the present systems. To test this hypothesis the $\beta$-hydride elimination of the $TiCl_3$-based edge site with a front side coordinated THF molecule on $MgCl_2$ was studied. The reaction was found to be extremely endothermic at 46.5 kcal/mol, and it was concluded that $\beta$-hydride elimination is unimportant also for the sites with a coordinated THF. Only the chain transfer with monomer reaction will be considered further here.

The transition states of hydrogen transfer to ethylene reaction were determined for all of the sites under considerations The energies of the transition states with respect to the appropriate $\pi$-complex ($E_{T(\pi)}$) and with respect to the separated ethylene and resting state ($E_{T(s)}$) are given in Table 7 and illustrated in Figures 11 and 12.

The termination barriers follow a pattern similar to those of the ethylene insertion reaction. The barriers with respect to the $\pi$-complexes are all fairly similar in magnitude being between 8 and 14 kcal/mol. The exception is the termination reaction when the growing polymer chain and the ethylene molecule are both on the back side of the slope site on $TiCl_2$, which has a significantly higher barrier of nearly 19 kcal/mol. Considering the barriers with respect to the separated site and monomer the calculated values for the edge sites are again generally lower than those of the slope sites and the barriers of the reaction when both the propyl group and the monomer are on the back side of the site are between 4 and 7 kcal/mol higher than for the other arrangements considered.

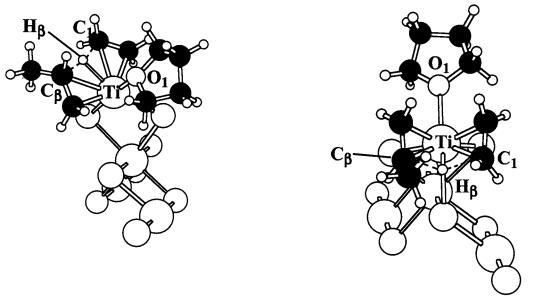


$C_1$-$H_\beta$=1.44Å Ti-$H_\beta$=1.89Å
$C_\beta$-$H_\beta$=1.49Å Ti-$O_1$=2.22Å

**a) Equatorial THF, axial ethylene**

$C_1$-$H_\beta$=1.56Å Ti-$H_\beta$=1.80Å
$C_\beta$-$H_\beta$=1.53Å Ti-$O_1$=2.28Å

**b) Front THF, back ethylene**

**Figure 12.** Chain transfer with ethylene transition states of the edge site.

**Table 8. Calculated Number Average Molecular Weights of Polymer Produced by Each Site Given the Calculated Insertion and Terminationi Barriers**

| site | $M_n$ |
|---|---|
| $MgCl_2$ surface | |
| slope | 32 000 |
| edge | 209 000 |
| $TiCl_2$ surface | |
| slope | 88 000 |
| edge | 7 600 000 |

The chain transfer with ethylene has a six-membered transition state which prefers to have all atoms in a plane (see Figures 11 and 12). This is more sterically demanding than the ethylene insertion reaction. As a result, the Ti to surface Cl bond was found to break in some of the calculations of the edge sites giving the structure in Figure 12a). The arrangement where both the propyl group and the ethylene molecule are on the back side of the site is so crowded that the coplanar transition state is no longer possible (Figures 11a and 12b) leading to a distorted and high energy geometry.

The combination of the insertion and termination reaction barriers can be used to calculate the molecular weight of the polymer produced at a given site. Taking the lowest insertion and termination barriers for each site, the number-average molecular weight of polymer that that site should produce at 350 K are given in Table 8.

The values in Table 8 depend on the exponential of the energy difference between the insertion and termination barriers and are thus very sensitive to changes in those barriers. The accuracy of the methods used here is of the order of a few kcal/mol and the quoted mass averages could therefore easily be off by 1 or 2 orders of magnitude. Even with this in mind, it is clear that catalysts as modeled here can all be described at "good" in the sense that they will produce polymer chains of a significant length. This is in contrast to the same sites without THF added. The polymer chains produced by many of these sites were predicted to be rather short.[31] The change in catalyst behavior is due to the increase in the barrier to termination upon addition of a THF molecule. The barrier to insertion is also increased by this change but it is increased less than that of termination. The reason for this difference is the fact that the transition state of insertion is less sterically demanding than that of termination, leading to a greater increase in the energy of the latter when the coordination number of Ti atom is increased.

## 5. Conclusions

In this paper the effects of the coordination of one or two molecules of THF to the proposed active sites of the $TiCl_4/MgCl_2$ Ziegler−Natta catalyst were examined.

All sites were found to bind THF exothermically with the reaction of the first THF molecule to a $TiCl_3$-based site being the most favorable. The interaction of THF with the aluminum−alkyl activator was also considered. Using the calculated reaction energies, equilibrium concentration distributions were obtained which suggest that unless a large excess of THF or aluminum−alkyl is present a single THF molecule coordinates almost all of the $TiCl_3$-based sites while almost none of the $TiCl_4$-based sites are affected. At the same time, a significant proportion of the aluminum−alkyl forms 1:1 complexes with the remaining THF molecules. In the presence of a large excess of THF the active sites do begin to become poisoned while in the presence of a large excess of aluminum−alkyl uncoordinated $TiCl_3$-based sites are formed.

The addition of a THF molecule to the coordination sphere of the Ti atom results in a poisoned active sites in the case of several of the models considered. For the remaining models the presence of THF decreases the $\pi$-complexation energy of ethylene and increases both the insertion and termination reaction barriers due to the increased steric crowding. However, since the transition state for termination is more sterically demanding than that of propagation the termination reaction is affected more leading to active sites that are less active but which produce polymer of higher molecular weight. This appears to be a general conclusion for all types of olefin-polymerization catalysts as a similar result has been found in computational studies of single site catalysts.[70,71]

If the equilibrium concentration distributions and modified reaction mechanisms are considered together a few further conclusions can be drawn. It appears that unless it is added in large excess THF will only poison one of the active site models. The $TiCl_3$-based Corradini site coordinates a single molecule THF strongly and is inactive once it has done so. The behavior of the $TiCl_4$-based sites will not be changed by the presence of THF, but the nonpoisoned $TiCl_3$-based sites will be less active but produce higher molecular weight polymer. Overall, the activity of the catalyst should decrease, but the mole fraction of the polymer corresponding to low molecular weight polymer will decrease in comparison to the fraction corresponding to higher molecular weight polymer.

**Acknowledgment.** We would like to thank Randal Ford and Jeff Vanderbilt for helpful discussions. We would also like to thank Eastman Chemical Company for financial support. T.Z. thanks the Canadian Government for a Canada Research Chair in Theoretical Inorganic Chemistry.

**Supporting Information Available:** Tables of Cartesian coordinates of all optimized structures. This material is available free of charge via the Internet at http://pubs.acs.org.

## References and Notes

(1) Barbé, P. C.; Cecchin, G.; Noristi, L. *Adv. Polym. Sci.* **1987**, *81*, 1.
(2) Galli, P.; Luciani, L.; Cecchin, G. *Angew. Makromol. Chem.* **1981**, *94*, 63.

(3) Boor, John J. *Ziegler−Natta Catalysts and Polymerizations*; Academic Press: New York, 1979.
(4) Chien, J. C.; Bres, P. *J. Polym. Sci., Polym. Chem. Ed.* **1986**, *24*, 1967.
(5) Giunchi, G.; Clementi, E.; Ruiz-Vizcaya, M. E.; Novaro, O. *Chem. Phys. Lett.* **1977**, *49*, 8.
(6) Novaro, O.; Blaisten-Barojas, E.; Clementi, E.; Giunchi, G.; Ruiz-Vizcaya, M. E. *J. Chem. Phys.* **1978**, *58*, 2337.
(7) Fujimoto, H.; Yamasaki, T.; Mizutani, H.; Koga, N. *J. Am. Chem. Soc.* **1985**, *107*, 6157.
(8) Sakai, S. *J. Phys. Chem.* **1994**, *98*, 12053.
(9) Sakai, S. *Int. J. Quantum Chem.* **1997**, *65*, 739.
(10) Colbourn, E. A.; Cox, P. A.; Carruthers, B.; Jones, P. J. V. *J. Mol. Catal.* **1994**, *4*, 805.
(11) Jensen, V. R.; Borve, K. J.; Ystenes, M. *J. Am. Chem. Soc.* **1995**, *117*, 9.
(12) Lin, J. S.; Catlow, C. R. A. *J. Mol. Catal.* **1993**, *3*, 1217.
(13) Lin, J. S.; Catlow, C. R. A. *J. Catal.* **1995**, *157*, 145.
(14) Cavallo, L.; Guerra, G.; Corradini, P. *J. Am. Chem. Soc.* **1998**, *120*, 2428.
(15) Monaco, G.; Toto, M.; Guerra, G.; Corradini, P.; Cavello, L. *Macromolecules* **2000**, *33*, 8953.
(16) Gale, J. D.; Catlow, C. R. A.; Gillan, M. J. *Top. Catal.* **1999**, *9*, 235.
(17) Puhakka, E.; Pakkanen, T. T.; Pakkanen, T. A. *Surf. Sci.* **1995**, *334*, 289.
(18) Puhakka, E.; Pakkanen, T. T.; Pakkanen, T. A. *J. Mol. Catal. A* **1997**, *120*, 143.
(19) Shiga, A.; Kawamura-Kuribayashi, H.; Sasaki, T. *J. Mol. Catal. A* **1995**, *98*, 15.
(20) Boero, M.; Parrinello, M.; Terakura, K. *J. Am. Chem. Soc.* **1998**, *120*, 2746.
(21) Boero, M.; Parrinello, M.; Hüffer, S.; Weiss, H. *J. Am. Chem. Soc.* **2000**, *122*, 501.
(22) Boero, M.; Parrinello, M.; Weiss, H.; Hüffer, S. *J. Phys. Chem. A* **2001**, *105*, 5096.
(23) Boero, M.; Parrinello, M.; Terakura, K.; Weiss, H. *Mol. Phys.* **2002**, *100*, 2935.
(24) Costuas, K.; Parrinello, M. *J. Phys. Chem. B* **2002**, *106*, 4477.
(25) Weiss, H.; Boero, M.; Parinello, M. *Macromol. Symp.* **2001**, *173*, 137.
(26) Toto, M.; Morini, G.; Guerra, G.; Corradini, P.; Cavallo, L. *Macromolecules* **2000**, *33*, 1134.
(27) Martinsky, C.; Minot, C. *Surf. Sci.* **2000**, *467*, 152.
(28) Martinsky, C.; Minot, C.; Ricart, J. *Surf. Sci.* **2001**, *490*, 237.
(29) Skalli, M. K.; Markovits, A.; Belmajdoub, A. *Catal. Lett.* **2001**, *76*, 7.
(30) Markovits, A.; Minot, C. *Int. J. Quantum Chem.* **2002**, *89*, 389.
(31) Seth, M.; Margl, P. M.; Ziegler, T. *Macromolecules* **2002**, *35*, 7815.
(32) Chadwick, J. C. In *Ziegler Catalysis*; Fink, G., Mülhaupt, R., Brintzinger, H. H., Eds.; Springer-Verlag: Berlin and Heidelberg, Germany, 1995; pp 427−440.
(33) Soga, K.; Shiono, T.; Doi, Y. *Makromol. Chem.* **1988**, *189*, 1531.
(34) Zakharov, V. A.; Makhtarulin, S. I.; Poluboyarov, V. A.; Anufrienko, V. F. *Makromol. Chem.* **1984**, *185*, 1781.
(35) Jones, P. J. V.; Oldman, R. J. In *Transition metals and organometallics as catalysts for olefin polymerization*; Kaminsky, W., Sinn, H., Eds.; Springer-Verlag: Berlin and Heidelberg, Germany, 1988; pp 223−229.
(36) Potapov, A. G.; Kriventsov, V. V.; Kochubey, D. I.; Bukatov, G. D.; Zakharov, V. A. *Macromol. Chem. Phys.* **1997**, *198*, 3477.
(37) Magni, E.; Somorjai, G. A. *Catal. Lett.* **1995**, *35*, 205.
(38) Magni, E.; Somorjai, G. A. *J. Phys. Chem.* **1996**, *100*, 14786.
(39) Kim, S. H.; Somorjai, G. A. *J. Phys. Chem. B* **2000**, *104*, 5519.
(40) Giannini, U. *Makromol. Chem. Suppl.* **1981**, *4*, 216.
(41) Corradini, P.; Barone, V.; Fusco, R.; Guerra, G. *Gazz. Chim. Ital.* **1983**, *113*, 601.
(42) Wychoff, R. W. G. *Crystal Structures*, 2nd ed.; John Wiley and Sons: New York, 1963; Vol. 1.
(43) Becke, A. D. *Phys. Rev. A* **1988**, *38*, 3098.
(44) Perdew, J. P. *Phys. Rev. B* **1986**, *33*, 8822.
(45) Vosko, S. H.; Wilk, L.; Nusair, M. *Can. J. Phys.* **1980**, *58*, 1200.
(46) ADF2000.01. Te Velde, G.; Bickelhaupt, F. M.; Baerends, E. J.; Fonseca Guerra, C.; Van Gisbergen, S. J. A.; Snijders, J. G.; Ziegler, T. *J. Comput. Chem.* **2001**, *22*.
(47) Baerends, E. J.; Ellis, D. E.; Ros, P. *Chem. Phys.* **1973**, *2*, 41.
(48) Versluis, L.; Ziegler, T. *J. Chem. Phys.* **1988**, *88*, 322.
(49) Te Velde, G.; Baerends, E. J. *Phys. Rev. B* **1991**, *44*, 7888.
(50) Fonseca Guerra, C.; Snijders, J. G.; Te Velde, G.; Baerends, E. J. *Theor. Chim. Acta* **1998**, *99*, 391.
(51) Dorrepaal, J. *Appl. Crystallogr.* **1984**, *17*, 483.
(52) Krijn, J.; Baerends, E. J. *Fit Functions in the HFS Method*; Technical Report; Department of Theoretical Chemistry, Free University: Amsterdam, The Netherlands, 1984.
(53) Clark, M.; Cramer, R D, I.; Van Opdenbosch, N. *J. Comput. Chem.* **1989**, *10*, 982.
(54) Rappé, A. K.; Casewit, C. J.; Colwell, K. S.; Goddard, W A, I.; Skiff, W. M. *J. Am. Chem. Soc.* **1992**, *114*, 10024.
(55) Berry, R. S.; Rice, S. A.; Ross, J. *Physical Chemistry*, 2nd ed.; Oxford University Press: New York, 2000, Chapter 19.
(56) Hehre, W. J.; Radom, L.; Schleyer, P. v.; Pople, J. A. *Ab Initio Molecular Orbital Theory*; Wiley: New York, 1986.
(57) Ochterski, J. W. *Thermochemistry in Gaussian*; Technical Report; Gaussian, Inc.: Pittsburgh, PA, 2000; http://www-.gaussian.com/thermo.htm.
(58) Willis, B. G.; Jensen, K. F. *J. Phys. Chem. A* **1998**, *102*, 2613.
(59) Wade, K. *J. Chem. Educ.* **1972**, *49*, 502.
(60) Henrickson, C. H.; Eyman, D. P. *J. Am. Chem. Soc.* **1989**, *111*, 1461.
(61) Matos, V.; Neto, A. G. M.; Nele, M.; Pinto, J. C. *J. Appl. Polym. Sci.* **2002**, *86*, 3226.
(62) *Handbook of Chmeistry and Physics*, 42nd ed.; Chemical Rubber Publishing Co.: Cleveland, OH, 1960.
(63) Odrian, G. *Principles of Polymerization*, 3rd ed.; John Wiley and Sons: New York, 1991.
(64) Chien, J. C.; Wu, J.-C.; Kuo, C.-I. *J. Polym. Sci., Polym. Chem. Ed.* **1982**, *20*, 2019.
(65) Cossee, P. *J. Catal.* **1964**, *3*, 80.
(66) Arlman, E. *J. Catal.* **1964**, *3*, 89.
(67) Arlman, E.; Cossee, P. *J. Catal.* **1964**, *3*, 99.
(68) Brookhart, M.; Green, M. L. H. *J. Organomet. Chem.* **1983**, *395*, 250.
(69) Lohrenz, J. C. W.; Woo, T. K.; Fan, L.; Ziegler, T. *J. Organomet. Chem.* **1995**, *497*, 91.
(70) Deng, L.; Woo, T. K.; Cavallo, L.; Margl, P. M.; Ziegler, T. *J. Am. Chem. Soc.* **1997**, *119*, 6177.
(71) Deng, L.; Ziegler, T.; Woo, T. K.; Margl, P.; Fan, L. *Organometallics* **1998**, *17*, 3240.

MA0301247